



1 **Determining the depth and pumping speed of the equatorial Ekman layer from**  
2 **surface drifter trajectories**

3

4 Nathan Paldor<sup>1</sup> and Yair De-Leon<sup>1</sup>

5

6 <sup>1</sup>Fredy and Nadine Herrmann Institute of Earth Sciences

7 Hebrew University of Jerusalem

8 Edmond J. Safra Campus, Givat Ram, Jerusalem, 9190401 Israel

9

10

11

12

13 Correspondence to: N. Paldor ([nathan.paldor@mail.huji.ac.il](mailto:nathan.paldor@mail.huji.ac.il))

14

15

16

17

18 **Abstract**

19 Trajectories of more than 500 drogued surface drifters launched since 1979 in the equatorial ocean are  
20 analyzed by employing the results of a new Lagrangian theory of wind-driven transport along the equator  
21 forced by the prevailing Trade winds. The analysis yields robust estimates of 45 meters for the Ekman  
22 layer's depth and 1.0 meters/day for the upwelling speed of deep water into the layer.



## 23 **1. Introduction**

24

25 The Trade winds that blow westward in the Tropics as part of the Hadley circulation are the first and basic  
26 component of the heat transport from the warm equatorial surface ocean to the cold poles, that  
27 mitigates the overall pole-to-equator temperature gradient on Earth. The mechanism that enables the  
28 poleward time-independent heat transport is the surface flow in the ocean that is directed  $90^\circ$  to the  
29 right/left of the wind in the northern/southern hemisphere relative to the direction of the overlying wind.  
30 This counter-intuitive flow direction results from Earth's rotation that adds the Coriolis force to the stress  
31 applied by the winds at the ocean surface. This straightforward scenario of wind-driven ocean circulation  
32 appears in all textbooks (Knauss, 1996; Talley et al., 2011) but despite its convincing simplicity, currently,  
33 no quantitative estimates are available for the parameters that control it.

34 The classical theory that describes the ocean response to forcing by the overlying winds was  
35 developed about 120 years ago by V.W. Ekman under the assumption of constant Coriolis frequency  
36 (Ekman, 1905). This assumption greatly simplifies the analysis by ensuring that all coefficients in the  
37 governing equations are constant. The dynamics described in Ekman's theory includes a steady flow  
38 perpendicular to the wind direction and inertial, i.e. force-free, oscillations at the local (constant) Coriolis  
39 frequency. This is in sharp contrast to the equatorial region where the Coriolis frequency vanishes at the  
40 equator and varies (linearly) with latitude, which turns the equations nonlinear so the oscillation-free  
41 flow is not steady as in Ekman's original mid-latitude theory. The poleward directed surface flows in both  
42 hemispheres along the equator imply a strong horizontal divergence along the equator which can only be  
43 balanced by the upwelling of deeper water into the wind-forced, Ekman, layer. Though the heuristic  
44 application of the mid-latitude Ekman theory to the vicinity of the equator is quite straightforward, to-  
45 date, the heuristic application could not be employed to estimate either the depth of the equatorial  
46 Ekman layer or the rate of upwelled volume of water.



47 The complications that result from the inclusion of the meridional variation of the Coriolis frequency in  
48 Ekman's theory were recently resolved in a theory of wind-driven flow in which Ekman's 1905 classical  
49 theory was extended to the equatorial region (Paldor, 2024). This new theory employs the adiabaticity  
50 method (Goldstein, 1980; Paldor and Friedland, 2023) to filter out the oscillation of a water column under  
51 the sole action of the meridionally varying Coriolis force from the slow and monotonic poleward motion  
52 of a water column forced by the combination of the wind stress and the Coriolis force. The essence of the  
53 method is the formulation of the problem as the dynamics of the motion of a (quasi-)particle about the  
54 minimum of a potential while the potential itself varies with time on a slower time scale than the period  
55 of oscillations about the minimum. The wind-driven dynamics along the equator can be transformed to  
56 this special form only by substituting the pseudo angular momentum for the zonal velocity component in  
57 the governing nonlinear equations (Paldor, 2024).

58 Direct observations of the depth (thickness) of the equatorial Ekman layer and the rate of upwelling  
59 water to it are not available due to the poor observational definition of the layer and the extremely low  
60 speed of upwelling. In contrast, observations of drifter trajectories are both abundant and accurate so  
61 they are used in the present study to estimate these important features of the equatorial Ekman layer  
62 using the new theory of wind-driven transport in the equatorial ocean. The application of this theory to  
63 drifter observations and the data used in this study are detailed in Section 2. In Section 3 we give the  
64 results obtained by applying the theory to drifter trajectories and the study is summarized in Section 4.

## 65 **2. Theory and Data**

### 66 **2.1. Theory**

67 The recent extension of the wind-driven theory of ocean circulation to the equator described in Paldor  
68 (2024) has demonstrated that, as in Ekman's original theory, the oceanic response can be decomposed  
69 into a monotonic, slow, flow (which is directed poleward in the equatorial region) and fast, large



70 amplitude, oscillations. In contrast to Ekman's original theory, in the equatorial region when the wind  
71 stress is directed westward the oscillations are highly nonlinear and of large amplitude (see Fig. 2 of  
72 Paldor, 2024). This new theory is applied in the present study to the trajectories of surface drifters by  
73 considering the dimensional counterpart of the non-dimensional expression derived in Eq. 9 of Paldor  
74 (2024) for the oscillation-free latitudinal motion of a water column or drifter launched near the equator:

$$75 \quad \frac{dy}{dt} = \frac{1}{y(t)} \frac{-\tau^x}{H} \left( \frac{R_e}{2\Omega\rho} \right). \quad (1)$$

76 Here,  $y(t)$  is the distance from the equator at time  $t$ . The global parameters in this relation are:  $\rho =$   
77  $1027 \text{ kg m}^{-3}$  (water density)  $\Omega = 7.29 \cdot 10^{-5} \text{ s}^{-1}$  and  $R_e = 6371 \cdot 10^3 \text{ m}$  (Earth's rotation frequency  
78 and radius, respectively) so  $\left( \frac{R_e}{2\Omega\rho} \right) = 4.25 \cdot 10^7 \text{ m}^4 \text{ s kg}^{-1}$ . The remaining, particular, parameters are:  $\tau^x$   
79 - the wind stress (units:  $\text{N m}^{-2}$ ; negative for easterly winds) and  $H$  (m) - the Ekman layer's depth.

80 Multiplying the nonlinear relation (1) by  $y(t)$  and integrating the resulting 1<sup>st</sup> order equation for  $y(t)^2$   
81 yields:

$$82 \quad y(t)^2 = y(0)^2 + 2 \frac{-\tau^x}{H} \cdot \left( \frac{R_e}{2\Omega\rho} \right) t. \quad (2)$$

83 Equation (2) can be applied to observations of drifter trajectories by inverting it to the following explicit  
84 expression for  $H$ :

$$85 \quad H = \left( \frac{R_e}{2\Omega\rho} \right) \frac{2(-\tau^x)}{L^2 - y_i(0)^2} t_i, \quad (3)$$

86 where  $y_i(0)$  is the distance of drifter # $i$  from the equator at  $t = 0$  (i.e. the distance of the launch point  
87 from the equator) and  $t_i$  is its travel time to  $L = y(t_i)$ , the final distance from the equator. The values of  
88  $H$  are calculated from this equation for each drifter and then averaged to yield the mean value for the  
89 particular value of  $L$ .



90 **2.2. Drifter trajectories**

91 Nearly 30,000 surface drifters were released from 1979 at the ocean surface (Lumpkin et al., 2017) and  
92 the geographical trajectories of these drifters are tracked by satellites every 6 hours for periods of up to  
93 1000 days. These (Lagrangian) observations cover the global ocean and a few percent of them were  
94 launched on both sides of the equator in the Pacific, Atlantic and Indian oceans. The slightly negatively  
95 buoyant drifter is typically drogued at 15-meter depth, so it provides an estimate of the current in the top  
96 15 meters of the water column where the wind stress is the primary forcing (Lumpkin et al., 2017). The  
97 agreement between drifter trajectories and ocean currents demonstrated in Lagerloef et al., (1999)  
98 motivates the analysis of observed trajectories of surface drifters in order to determine the depth of the  
99 equatorial Ekman layer and the pumping (upwelling) speed of deep water into it.

100 The drifter trajectories used in the analysis were collected and made freely available by the NOAA  
101 Global Drifter Program (NOAA/GDP). The data were screened according to the following three criteria:

- 102 1. They were launched within  $1^\circ \approx 110$  km south or north of the equator (regarded as the equator).
- 103 2. The drifters remained in one hemisphere throughout the entire travel time to the final latitude  
104 (equator crossing is not allowed under westward directed wind stress).
- 105 3. The drifters were continuously tracked, with gaps no longer than one day, during their motion from  
106 the launch point to the final latitude that marks the boundary of the equatorial region (i.e.  $3^\circ \approx$   
107  $330$  km,  $4^\circ \approx 440$  km or  $5^\circ \approx 550$  km).

108 The latitudes  $3^\circ$  and  $4^\circ$  were used in previous studies to define the boundaries of the equatorial region  
109 (Brady and Bryden, 1987; Lagerloef et al., 1999; Johnson et al., 2001) but in the present study we also  
110 used  $L = 5^\circ \approx 550$  km to verify the robustness of the calculated averages to the selected values of  $L$ . For  
111  $L = 2^\circ \approx 220$  km the singularity at  $L^2 \rightarrow y_i(0)^2$  in Eq. (3) yields highly erratic and too high value of  $H$ .

112 Of the nearly 30,000 drifter trajectories archived in AOML archive as of 8/2024, over 1500 drifters  
113 reached the final latitude ( $3^\circ$ ,  $4^\circ$  or  $5^\circ$ ) and out of them about 700 drifters remained in one hemisphere.



114 The number of drifters in the Atlantic and Pacific oceans that reached each of the final latitude is given in  
 115 the 2<sup>nd</sup> column of Table 1 that includes, in addition, the mean launch distances of  $y_i(0)$  (3<sup>rd</sup> column) and  
 116 mean travel times of  $t_i$ , (4<sup>th</sup> column) to the final latitudes (noted in the rows of this table). The Indian  
 117 Ocean is excluded from the analysis due to its positive mean annual wind stress (see Sect. 2.3).

### 118 2.3. Wind stress

119 The daily wind stress values over the oceans,  $\tau^x$ , used in this work are available at NOAA/CoastWatch site  
 120 in 0.125° spatial resolution for the period 1999-2009. We calculated the averaged wind stress in the  
 121 region of the Indian, Atlantic and Pacific oceans in a zonal strip that straddles the equator between  $-L$   
 122 and  $+L$ , where  $L$  corresponds to 3°, 4° or 5°. These averages are given in the 5<sup>th</sup> column of Table 1 for the  
 123 Atlantic and Pacific oceans but not for the Indian ocean where the calculated mean values are positive (so  
 124  $H < 0$ ) and small (less than  $+0.01 \text{ N m}^{-2}$ ) probably due to the strong seasonal forcing by the Monsoon  
 125 system that induces eastward directed zonal winds throughout part of the year in this ocean (Hastenrath  
 126 and Polzin, 2004; Zhang et al., 2022).

$L$ (degrees)	Number of drifters	Mean $y_i(0)$ (degrees)	Mean $t_i$ (days)	$\tau^x$ ( $\text{Nm}^{-2}$ )	Mean $H$ (m)	$W = \frac{H}{t_i} \cdot \frac{L - y_i(0)}{L}$ (m/day)
3.04	610	0.29	29.67	-0.0261	51.10	1.56
4.04	576	0.29	43.43	-0.0264	42.48	0.91
5.04	531	0.29	58.12	-0.027	37.16	0.60

127

128 **Table 1: Drifter characteristics in the Pacific and Atlantic oceans and the zonal wind stresses there. The**  
 129 **shown values of  $L$  are larger by a few kilometers compared to the distances corresponding to 3°, 4° or**  
 130 **5° since a drifter is determined to be “at  $L$ ” with an offset of up to 6 hours after its passage of that**  
 131 **point. Less than 10% percent of the relevant drifters were launched in the Indian ocean which is not**  
 132 **included in this table and in the analysis since the annual mean wind stress in the Indian Ocean is**  
 133 **directed eastward, which is inconsistent with a poleward directed net motion.**

### 134 3. Results



135 Four representative drifter trajectories are shown in Fig. 1 and they demonstrate the richness of observed  
136 trajectories near the equator, the intricate combination of oscillations with slow poleward propagation  
137 and the occurrence of equatorial crossing in many trajectories.

138 Substituting the values of  $y_i(0)$  and  $t_i$  for each drifter in Eq. (3) and averaging these values over all  
139 relevant drifters yields the values of  $H$  given in the 6<sup>th</sup> column of Table 1. The histograms of the  $H$  values  
140 for each value of  $L$  are shown in Fig. 2 so the value of  $H$  is best estimates by:  $H = 44 \pm 7 \approx 45$  m.

141 Equation (2) can also be employed to calculate the poleward, oscillation-free, velocity of a drifter on  
142 its way from  $y_i(0)$  to  $L = y(t_i)$  from the drifter's average speed during its travel:  $V = \frac{L-y_i(0)}{t_i}$ . Thus, the

143 volume divergence (per unit length in  $x$ ) that results from the anti-parallel, poleward directed, volume  
144 fluxes of 2 water columns that are initially conjoined along the equator and move poleward is  $2HV =$   
145  $2H \frac{L-y_i(0)}{t_i}$ . The vertical volume flux (per unit length) due to Ekman pumping during  $t_i$  is:  $2LW$ , where  $W$

146 is the pumping speed. Equating the vertical and horizontal fluxes yields  $WL = H \frac{L-y_i(0)}{t_i}$  or  $W = \frac{H}{L} \frac{L-y_i(0)}{t_i}$ .

147 The mean values of  $H$  and  $t_i$  in Table 1 then yield the mean value of  $W \approx 1.0$  m/day for the three values  
148 of  $L$ .

149 The estimated  $H$  and  $W$  values along the equatorial Atlantic and Pacific Oceans are noted in Fig. 3 on a  
150 qualitative, textbook, cartoon of the wind forcing and resulting oceanic flow patterns.

#### 151 **4. Summary and Discussion**

152 The mean estimates  $H = 45$  m and  $W = 1$  m/day calculated here based on surface drifter trajectories  
153 are more robust compared to prior estimates derived from standard hydrographic observations. Table 1  
154 shows that the present estimates of  $H$  vary with  $L$  by a few meters and those for  $W$  by about  $0.5 \frac{m}{day}$ .

155 These variations are smaller than those of estimates based on standard hydrographic data that can vary  
156 by a factor of up to 3 (Wyrтки, 1981; Brady and Bryden, 1987; Lukas and Lindstrom, 1991; Weingartner



157 and Weisberg, 1991). As an example, the  $H = 45 \text{ m}$  value reported here exceeds the estimate of 30-40 m  
158 proposed in Lukas and Lindstrom (1991) but the  $O(10\%)$  variation of the present estimate is significantly  
159 smaller than  $O(80\%)$  variation in the latter estimate. In view of the crucial role played by the poleward  
160 flow of warm equatorial water in mitigating the large radiative pole-to-equator temperature gradient  
161 (Czaja and Marshal, 2006; Hartmann, 2016) a reliable quantification of the initiation of this flow is  
162 important for understanding Earth's climate.

163 The successful application of the new theory of wind-driven equatorial transport in the ocean  
164 developed in Paldor (2024) lends credence to the relevance of this theory to observations in the  
165 equatorial ocean. It can be argued that the calculation and successful application of the oscillation-free  
166 speed of poleward wind-driven motion on the equator is of similar significance to ocean dynamics as the  
167 development of the expression for the steady transport in the original  $f$ -plane Ekman theory.

168

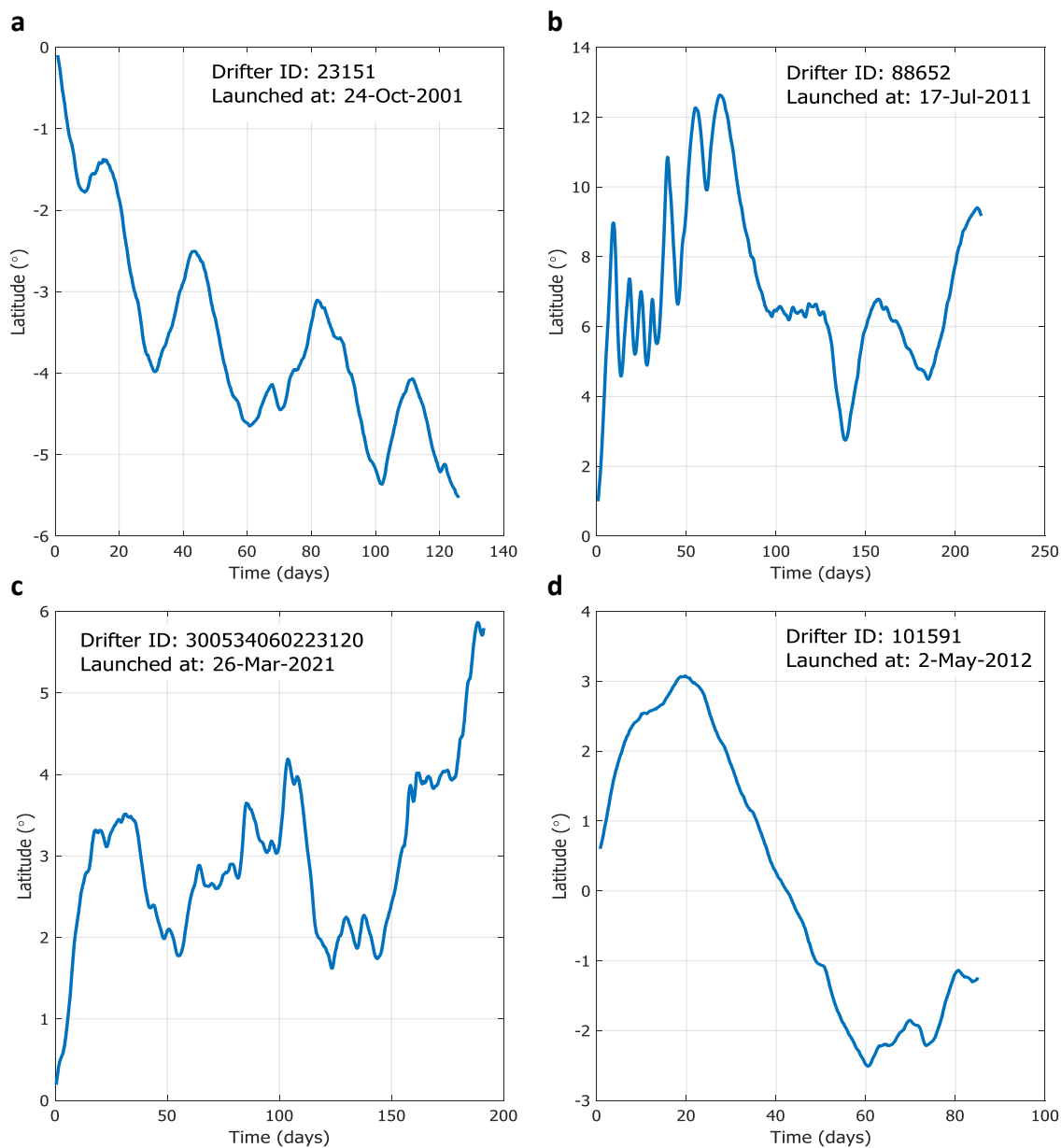
169 **Author contribution:**

170 NP: Initiation of project, writing various drafts and theoretical analysis

171 YD: Data collection and analysis, editing and production of display items.

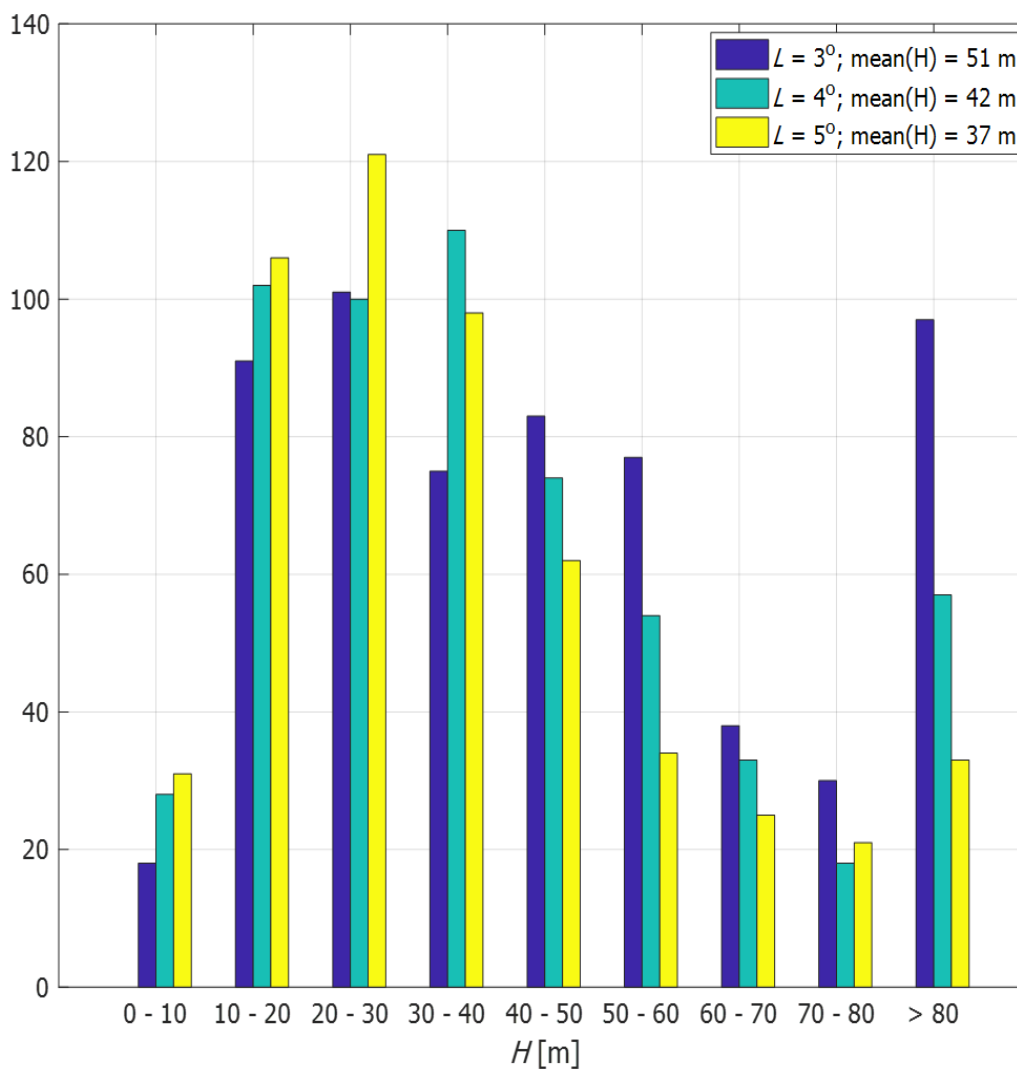
172 **Competing interests:** The authors declare that they have no conflict of interest.

173 **Financial support:** The authors happily declare that no funding was received for this study



174 **Figure 1: Four drifter trajectories originating within 1° of the equator analyzed in this study. a) A typical**  
175 **southern hemisphere trajectory that clearly shows oscillations and a mean poleward flow; b) A fast**  
176 **northern hemisphere trajectory that reaches 4° in just a few days; c) A slow northern hemisphere**  
177 **trajectory that reaches 4° in more than 100 days; d) A trajectory that reaches 3° but not 4° prior to**  
178 **crossing the equator so it is included in the analysis of  $L = 3^\circ$  since it crosses the equator only after**  
179 **reaching 3° N.**

180

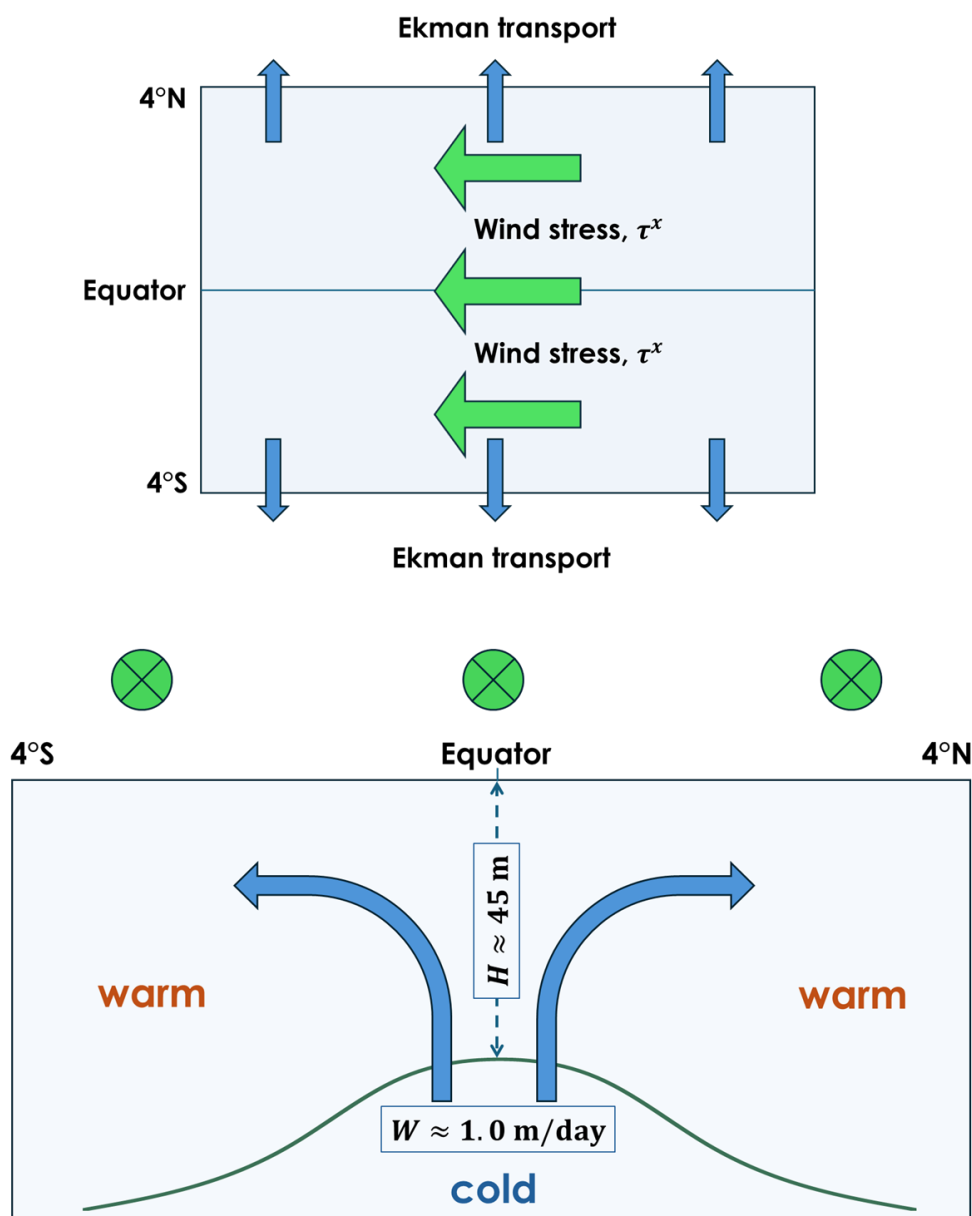


181

182 **Figure 2: The histograms of  $H$ -values for the 3 values of  $L$ . For  $L = 3^\circ$  the tail of  $H > 80$  m is as high as**  
183 **the maximum cell of  $H = 20 - 30$  m consistent with singularity of Eq. (3) at  $L^2 \approx y_i(0)^2$ .**



184



185

186 Figure 3: A sketch relating the poleward directed wind-driven surface flow along the equator under  
187 westward directed wind stress (upper panel) which is compensated by the upwelling of water from  
188 below (lower panel). The upper panel is a planar view and the lower panel is a latitude-height cross-  
189 section viewed from the east. The  $H \approx 45$  m and  $W \approx 1.0$  m/day estimates are the main results of  
190 this study.



## 191 References

- 192 Brady, E. C. and Bryden, H. L.: Estimating vertical velocity on the Equator. *Oceanologica Acta, Special*  
193 *Issue*, 1987.
- 194 Czaja, A. and Marshall, J.: The partitioning of poleward heat transport between the atmosphere and  
195 ocean. *J. Atm. Sci.*, **63(5)**, 1498-1511. <https://doi.org/10.1175/JAS3695.1>, 2006.
- 196 Ekman, V. W.: On the influence of earth's rotation on ocean-currents. *Ark. Mat. Astr. Fys.*, **2**, 1–52, 1905.
- 197 Goldstein, H.: *Classical Mechanics*. Addison-Wesley, Inc, 1980.
- 198 Hartmann, D. L.: *Global Physical Climatology*, 2<sup>nd</sup> Ed., Elsevier Inc. [https://doi.org/10.1016/C2009-0-](https://doi.org/10.1016/C2009-0-00030-0)  
199 [00030-0](https://doi.org/10.1016/C2009-0-00030-0), 2016.
- 200 Hastenrath, S. and Polzin, D.: Dynamics of the surface wind field over the equatorial Indian Ocean. *Q. J. R.*  
201 *Meteorol. Soc.*, **130**, 503-517. <https://doi.org/10.1256/qj.03.79>, 2004.
- 202 Johnson, G. C., McPhaden, M. J., and Firing, E.: Equatorial Pacific Ocean Horizontal Velocity, Divergence,  
203 and upwelling. *J. Phys. Oceanogr.*, **31(3)**, 839-849. [https://doi.org/10.1175/1520-](https://doi.org/10.1175/1520-0485(2001)031<0839:EPOHVD>2.0.CO;2)  
204 [0485\(2001\)031<0839:EPOHVD>2.0.CO;2](https://doi.org/10.1175/1520-0485(2001)031<0839:EPOHVD>2.0.CO;2), 2001.
- 205 Krauss, J. A.: *Introduction to Physical Oceanography*, 2<sup>nd</sup> Ed. Prentice Hall, Inc. ISBN 0-13-238155-9, 1996.
- 206 Lagerloef, G. S. E., Mitchum, G. T., Lukas, R. B. and Niiler, P. P.: Tropical Pacific near-surface currents  
207 estimated from altimeter, wind, and drifter data. *J. Geophys. Res.: Oceans*, **104(10)**, 23,313-23,326.  
208 <https://doi.org/10.1029/1999JC900197>, 1999.
- 209 Lukas, R. and Lindstrom, E.: The mixed layer of the western equatorial Pacific Ocean *J. Geophys. Res.:*  
210 *Oceans*. **96**, 3343-3357. <https://doi.org/10.1029/90JC01951>, 1991.
- 211 Lumpkin, R., Ozgokmen, T. and Centurioni, L.: Advances in the application of surface drifters. *Ann. Rev.*  
212 *Mar. Sci.*, **9**, <https://doi.org/10.1146/annurev-marine-010816-060641>, 2017.
- 213 [NOAA/CoastWatch](https://coastwatch.pfeg.noaa.gov/erddap/files/erdQStress3day/erdQStaux3day/): <https://coastwatch.pfeg.noaa.gov/erddap/files/erdQStress3day/erdQStaux3day/>
- 214 NOAA/GDP: [https://erddap.aoml.noaa.gov/gdp/erddap/tabledap/drifter\\_6hour\\_qc.html](https://erddap.aoml.noaa.gov/gdp/erddap/tabledap/drifter_6hour_qc.html)
- 215 Paldor, N. and Friedland, L.: Wind-driven transport of the spherical earth. *Phys. Fluids*, **35**, 056604.  
216 <https://doi.org/10.5194/os-19-93-2023>, 2023.
- 217 Paldor, N.: A Lagrangian theory of equatorial upwelling. *Phys. Fluids*, **36**, 046605.  
218 <https://doi.org/10.1063/5.0202412>, 2024.
- 219 Talley, L. D., Pickard, G. L., Emery, W. J. and Swift, J. H.: *Descriptive Physical Oceanography: An*  
220 *Introduction*, 6<sup>th</sup> Ed. Academic Press. ISBN: 978-0-7506-4552-2, 2011.
- 221 Weingartner, T. J. and Weisberg, R. H.: On the annual cycle of equatorial upwelling in the central Atlantic  
222 Ocean, *J. Phys. Oceanogr.*, **21(1)**, 68-82. [https://doi.org/10.1175/1520-](https://doi.org/10.1175/1520-0485(1991)021<0068:OTACOE>2.0.CO;2)  
223 [0485\(1991\)021<0068:OTACOE>2.0.CO;2](https://doi.org/10.1175/1520-0485(1991)021<0068:OTACOE>2.0.CO;2), 1991.
- 224 Wyrtki, K.: An estimate of equatorial upwelling in the Pacific. *J. Phys. Oceanogr.* **11(9)**. 1205-1214.  
225 [https://doi.org/10.1175/1520-0485\(1981\)011<1205:AEOEUI>2.0.CO;2](https://doi.org/10.1175/1520-0485(1981)011<1205:AEOEUI>2.0.CO;2), 1981.
- 226 Zhang, L., Li, Y. and Li, J.: Impact of equatorial wind stress on Ekman transport during the mature phase of  
227 the Indian Ocean Dipole. *Clim. Dyn.* **59**, 1253–1264. <https://doi.org/10.1007/s00382-022-06183-7>,  
228 2022.